© The American Society of Gene & Cell Therapy

Comparative Study of Liver Gene Transfer With AAV Vectors Based on Natural and Engineered AAV Capsids

Lili Wang[1], Peter Bell[1], Suryanarayan Somanathan[1], Qiang Wang[1], Zhenning He[1], Hongwei Yu[1], Deirdre McMenamin[1], Tamara Goode[1], Roberto Calcedo[1] and James M Wilson[1]

[1]*Gene Therapy Program, Department of Pathology and Laboratory Medicine, University of Pennsylvania Perelman School of Medicine, Philadelphia, Pennsylvania, USA*

Vectors based on the clade E family member adeno-associated virus (AAV) serotype 8 have shown promise in patients with hemophilia B and have emerged as best in class for human liver gene therapies. We conducted a thorough evaluation of liver-directed gene therapy using vectors based on several natural and engineered capsids including the clade E AAVrh10 and the largely uncharacterized and phylogenically distinct AAV3B. Included in this study was a putatively superior hepatotropic capsid, AAVLK03, which is very similar to AAV3B. Vectors based on these capsids were benchmarked against AAV8 and AAV2 in a number of *in vitro* and *in vivo* model systems including C57BL/6 mice, immune-deficient mice that are partially repopulated with human hepatocytes, and nonhuman primates. Our studies in nonhuman primates and human hepatocytes demonstrated high level transduction of the clade E-derived vectors and equally high transduction with vectors based on AAV3B. In contrast to previous reports, AAVLK03 vectors are not superior to either AAV3B or AAV8. Vectors based on AAV3B should be considered for liver-directed gene therapy when administered following, or before, treatment with the serologically distinct clade E vectors.

Received 3 June 2015; accepted 17 August 2015; advance online publication 27 October 2015. doi:10.1038/mt.2015.179

INTRODUCTION

Liver is the desired target for gene transfer in the treatment of a variety of inherited diseases. A number of viral and nonviral vectors have been evaluated for liver-directed gene therapy, although vectors based on adeno-associated viruses (AAV) show the most promise.[1] Initial work utilized vectors based on AAV serotype 2 to treat hemophilia B.[2–5] However, in clinical trials, transduction of hepatocytes was low and transgene expression was transient.[6]

Initial attempts to improve performance of AAV2 vectors used capsids from the other five capsid serotypes that had been isolated in the 1960s as contaminants of primate adenoviruses.[7,8] The results were mixed with some capsids demonstrating improved transduction of tissues other than liver. We created vectors based on AAV1 that showed improved transduction of skeletal and cardiac muscle forming the basis of a commercially approved product (*i.e.*, Glybera).[9,10] The utility of AAV vectors was expanded by the Wilson Laboratory through the isolation of over 100 natural capsid variants from human and nonhuman primates, some of which showed substantial improvements in targeting liver.[11] A systematic evaluation of these novel capsids in mice and nonhuman primates identified AAV8 as the preferred capsid for liver-directed gene therapy.[12–14] Hemophilia B patients treated with an AAV8 vector showed dose-dependent expression of factor IX that has been stable for at least 4–5 years; this has reduced and in some cases eliminated the requirement for protein replacement.[15,16] Two other capsids isolated from primate tissues, AAVrh10 and AAV9, are in the clinic for treating several neurodegenerative diseases.[17–19]

More recent attempts to improve vector performance have used existing AAV capsids to create diverse populations of engineered variants that are propagated under selective pressure to isolate those with the desired property, which in most cases is improved transduction.[20–26] The challenge is establishing a selection system that recapitulates *in vivo* delivery in humans. These capsid variants show promise in model systems, although none have progressed to the clinic.

In an attempt to broaden the repertoire of capsids for liver gene therapy, we conducted a thorough evaluation of vectors based on two previously described endogenous capsids, AAVrh10 and AAV3B, as well as the recently described engineered capsid AAVLK03,[26] all of which were benchmarked against AAV2 and AAV8.

RESULTS

AAVrh10 was selected for this study because it is emerging as a lead capsid for clinical applications outside of the liver.[17,18] The expectation is that vectors based on AAVrh10 will have similar properties to AAV8 vectors since they are both from clade E and differ by only 8% in terms of the amino acid sequence of VP3. As shown in **Figure 1**, these differences are localized primarily to the surface exposed hypervariable regions. AAV3B is quite distinct structurally and serologically from AAV8 (see **Figure 1** for summary of structural differences). Interestingly, capsids similar to AAV3B have rarely been recovered from natural sources, with the exception of one named as AAV (VR-942), which was isolated

Correspondence: James M. Wilson, Gene Therapy Program, Department of Pathology and Laboratory Medicine, University of Pennsylvania, Philadelphia, Pennsylvania 19104, USA. E-mail: wilsonjm@mail.med.upenn.edu

© The American Society of Gene & Cell Therapy

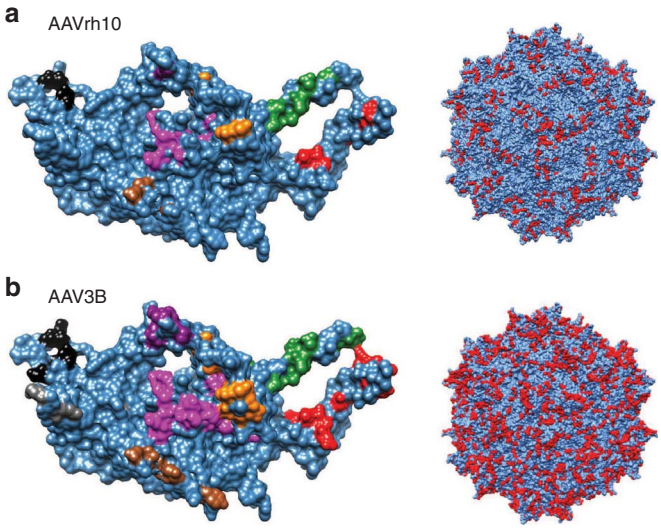

Figure 1 Structural comparison of adeno-associated virus (AAV) 8 with AAVrh10 and AAV3B. Surface rendering of the VP3 subunit illustrating the differences between AAV8 and AAVrh10 (**a**) and AAV8 and AAV3B (**b**). In the left part of each panel, different colors indicate the differences in hypervariable regions I–IX relative to the AAV8 VP3 monomer (PDB: 2QA0).[44] In the right part of each panel, the differences on the surface of the capsid are shown in red. The models are generated with Chimera program.[45,46]

by polymerase chain reaction (PCR) as a contaminant of simian adenovirus 17.[27] The closest family to AAV3B is clade C, which is a collection of viruses formed from an AAV2/AAV3 hybrid. Not much work has been conducted with vectors based on AAV3B because of very low *in vivo* transduction efficiencies in murine models. However, Srivastava and co-workers have shown high transduction of human hepatoma cell lines with vectors based on AAV3.[28–30] Lisowski *et al.*[26] used a human liver xenograft model (*i.e.*, an immune deficient mouse in which human hepatocytes partially repopulate the liver) to select for an AAV capsid variant from a shuffled library that demonstrated high human hepatocyte tropism. This engineered capsid, called AAVLK03, is very similar to AAV3B with only eight amino acid differences between the two capsids, only one of which is located in the VP3 protein. A figure in the patent that describes the work of Lisowski and Kay[31] indicated a sequence for AAVLK03 different from the sequence in the paper. This sequence variant, which we call AAVLK03.L125I, differs from AAVLK03 by the presence of an Ile (same as it is in AAV3B) rather than a Leu at position 125 in VP1. Since this is a conserved amino acid difference buried in the scaffold of the capsid and not exposed to the surface, it is unlikely to impact the function of the capsid. Despite the high probability of equivalency between these two capsids, we decided to conduct parallel experiments with AAVLK03 and AAVLK03.L125I. For purposes of this report, AAV8 and AAVrh10 are referred to as "clade E vectors" while AAV3B, AAVLK03, and AAVLK03.L125I are referred to as "AAV3-related vectors".

Vectors expressing LacZ were evaluated for transduction of the human hepatoma cell line Huh7 at MOIs of 1,000 and 10,000 (**Supplementary Figure S1**). As has been previously noted, *in vitro* transduction with AAV3B is high, versus low with AAV8;[11,29] transduction with AAVrh10 was indistinguishable from

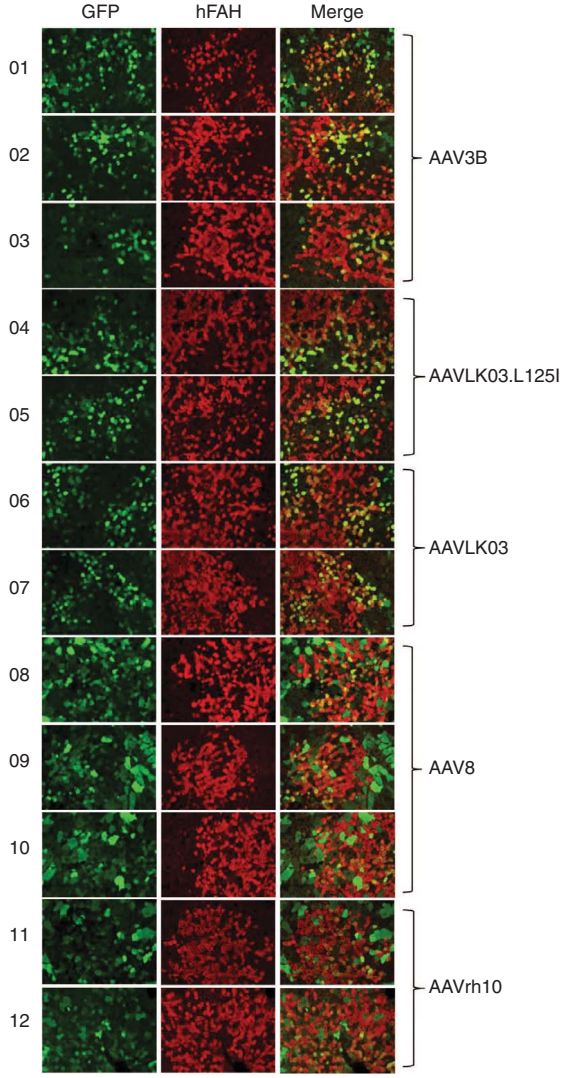

Figure 2 Differential transduction of human and mouse hepatocytes by adeno-associated virus (AAV) vectors. FRG mice were transduced with 3×10^{11} GC of AAV vectors expressing green fluorescent protein (GFP). Livers were isolated from animals 21 days postvector administration, sectioned and stained for human fumaryl acetoacetate hydrolase (hFAH, red color). Images were obtained using a Nikon inverted microscope using a 20× objective and equipped with a digital camera. A digital merge of the GFP and hFAH images is shown on the right panels.

that of AAV8. AAVLK03 and AAVLK03.L125I vectors showed transduction efficiencies equivalent to AAV3B, which is at variance with the findings of Lisowski *et al.*, where transduction of Huh7 cells with AAVLK03 vectors was shown to be 43-fold higher than with AAV3B vectors.[26]

All *in vivo* studies were conducted with vectors expressing green fluorescence protein (GFP) from the liver-specific TBG promoter. This allowed for an assessment of transduction efficiency using fluorescent microscopy and overall transgene expression by direct measure of GFP protein from liver homogenates. Expression studies were therefore limited to times of necropsy; sequential measures over time were not possible as would be the case if a secreted transgene product was used. Initial studies were conducted in C57BL/6 mice injected intravenously (IV)

Sarepta Exhibit 1071, page 2

© The American Society of Gene & Cell Therapy

with different doses of vector. At a dose of 1×10^{11} GC/mouse, the two clade E capsids, AAVrh10 and AAV8, demonstrated very high transduction of hepatocytes (84 and 81%, respectively) while AAV3B, AAVLK03, and AAVLK03.L125I vectors poorly transduced mouse hepatocytes (0.1, 3.9, and 2.5%, respectively). These data are consistent with previous reports of high transduction in mouse liver *in vivo* of clade E vectors and low transduction of AAV3B and AAVLK03.[12,26]

Table 1 Differential transduction of human and mouse hepatocytes by AAV vectors[a]

		% Transduction (FACS)[b]		% Transduction (morphometric)[c]	
Vector	Mouse	Human (MFI)	Mouse (MFI)	Human	Mouse
AAV3B	01	26 (1.5E+5)	6 (1.3E+5)	21 ± 7	6 ± 2
AAV3B	02	19 (8.3E+4)	10 (1.3E+5)	31 ± 11	12 ± 7
AAV3B	03	24 (6.1E+4)	6 (1.0E+5)	17 ± 6	1 ± 0.4
AAVLK03.L125I	04	28 (5.3E+4)	8 (9.0E+4)	38 ± 17	13 ± 6
AAVLK03.L125I	05	28 (7.1E+4)	12 (1.1E+5)	36 ± 11	9 ± 3
AAVLK03	06	30 (4.8E+4)	15 (6.9E+4)	31 ± 8	5 ± 3
AAVLK03	07	32 (1.3E+5)	17 (5.1E+4)	17 ± 7	6 ± 3
AAV8	08	n/a	n/a	16 ± 9	16 ± 4
AAV8	09	61 (7.3E+4)	42 (1.3E+5)	25 ± 10	27 ± 4
AAV8	10	32 (6.7E+4)	28 (6.3E+4)	39 ± 10	51 ± 7
AAVrh10	11	23 (4.1E+4)	14 (4.0E+4)	19 ± 11	23 ± 4
AAVrh10	12	58 (6.5E+4)	27 (8.5E+4)	38 ± 14	42 ± 12

[a]Differential transduction of human and mouse hepatocytes was evaluated by flow cytometric analysis of isolated hepatocytes (FACS) or by sectioning whole livers (morphometry). [b]For FACS, the transduced GFP-positive subset and the mean fluorescent intensity (MFI) among the human or mouse hepatocytes is presented. [c]For morphometric analysis, individual liver sections were stained with an anti-human FAH antibody to differentiate human and mouse cells. The percent area (pixels) of GFP expression among human (GFP+/hFAH+) or mouse cells (GFP+/hFAH–) is presented along with standard deviation.
n/a, data was not available.

In an attempt to better model transduction of human liver, we utilized the *Fah*$^{-/-}$ /*Rag*$^{-/-}$ /*Il2rg*$^{-/-}$ (FRG) mouse in which the liver from this immune deficient mouse is partially repopulated with human hepatocytes (subsequently called the human liver xenograft model).[32–34] Following IV injection of GFP-expressing vector into the human liver xenograft model, we harvested liver and quantified transduction of endogenous mouse and human hepatocytes using two different approaches. The standard method is based on the immunofluorescence analysis of liver tissue sections looking for colocalization of transgene expression with a cell-specific marker for the engrafted human hepatocytes (*i.e.*, human fumarylacetoacetase (hFAH)). Morphometric analyses of these experiments revealed the following populations of cells: transduced human hepatocytes—GFP$^+$ hFAH$^+$; non-transduced human hepatocytes—GFP$^-$ hFAH$^+$; transduced mouse cells—GFP$^+$ hFAH$^-$, and nontransduced mouse hepatocytes—GFP$^-$ hFAH$^-$. **Figure 2** presents representative fluorescent micrographs of liver harvested from human liver xenograft mice 3 weeks after injection with 3×10^{11} GC of AAV.TBG.GFP. In this analysis, green represents GFP-expressing cells, red represents hFAH-expressing cells, and yellow represents cells expressing both markers. The remaining part of each liver was subjected to a second method for quantitating transduction based on flow cytometric analysis of single cell suspensions of hepatocytes released following perfusion with collagenase and staining with antibodies for mouse (H2-k^b) and human (HLA) cells. Transduction efficiencies were measured by colocalization of GFP with the cell-specific markers. A summary of mouse xenograft studies in terms of transduction efficiencies using both methods is provided in **Table 1**.

Table 2 Summary of gene transfer in macaques after systemic vector administration

				GFP transduction in liver			GFP DNA copy/ diploid genome[e]		
Vector serotype	Animal no.	Pre AAV Nab (1:dilution)	Capsid in spleen[a]	Efficiency (%)[b] (mean ± SD)	Intensity[c] (mean ± SD)	GFP protein[d] (ng/μg protein)	Liver	Spleen	Spleen/ liver GFP DNA ratio
AAV3B	RQ9759	<1:5	++	25.6 ± 5.6	1.02 ± 0.27	0.73	17.1	9.6	0.56
	RQ9831	<1:5	++	24.4 ± 17.2	1.16 ± 0.19	0.65	13.1	19.6	1.50
AAVLK03. L125I	RQ8982	<1:5	+++	17.8 ± 9.2	0.66 ± 0.14	0.49	7.0	30.9	4.4
	RQ9284	<1:5	+++	3.8 ± 1.8	0.51 ± 0.09	0.12	1.2	31.0	25.8
AAVLK03	RQ9828	<1:5	++	15.2 ± 9.0	0.43 ± 0.07	0.18	0.5	34.0	68.0
	RQ9837	1:20	++	0.1 ± 0.1	0.31 ± 0.04	0	0.003	25.3	8433.3
AAVrh10	090-0266	<1:5	+	14.5 ± 10.1	0.47 ± 0.11	0.18	9.6	7.1	0.74
	090-0283	<1:5	+/–	15.8 ± 7.0	0.58 ± 0.21	0.45	20.1	9.4	0.47
AAV8	RQ8082	<1:5	+	23.0 ± 17.6	0.79 ± 0.26	0.45	26.2	2.8	0.11
	RQ8083	<1:5	–	20.5 ± 12.7	0.92 ± 0.24	0.47	29.4	3.0	0.10
AAV2	03D313	<1:5	++	1.6 ± 1.8	0.35 ± 0.04	0.12	28.8	28.5	0.99

AAV, adeno-associated virus; GFP, green fluorescent protein; NAb, neutralizing antibody.
[a]Detection of capsid protein in spleen by immunofluorescence. [b]Measured as the percentage of GFP-positive area per liver section regardless of brightness. Ten sections per animal were analyzed. [c]Determined as the total intensity of each image with background level subtracted (see Materials and Methods). Ten sections per animal were analyzed. [d]Determined by an enzyme-linked immunosorbent assay on liver lysate. [e]Determined by quantitative polymerase chain reaction of transgene GFP, according to a standard curve generated with linearized plasmid DNA, pAAV.CMV.GFP. The limit of detection is 7×10^{-5} copies/diploid genome.

Sarepta Exhibit 1071, page 3

© The American Society of Gene & Cell Therapy

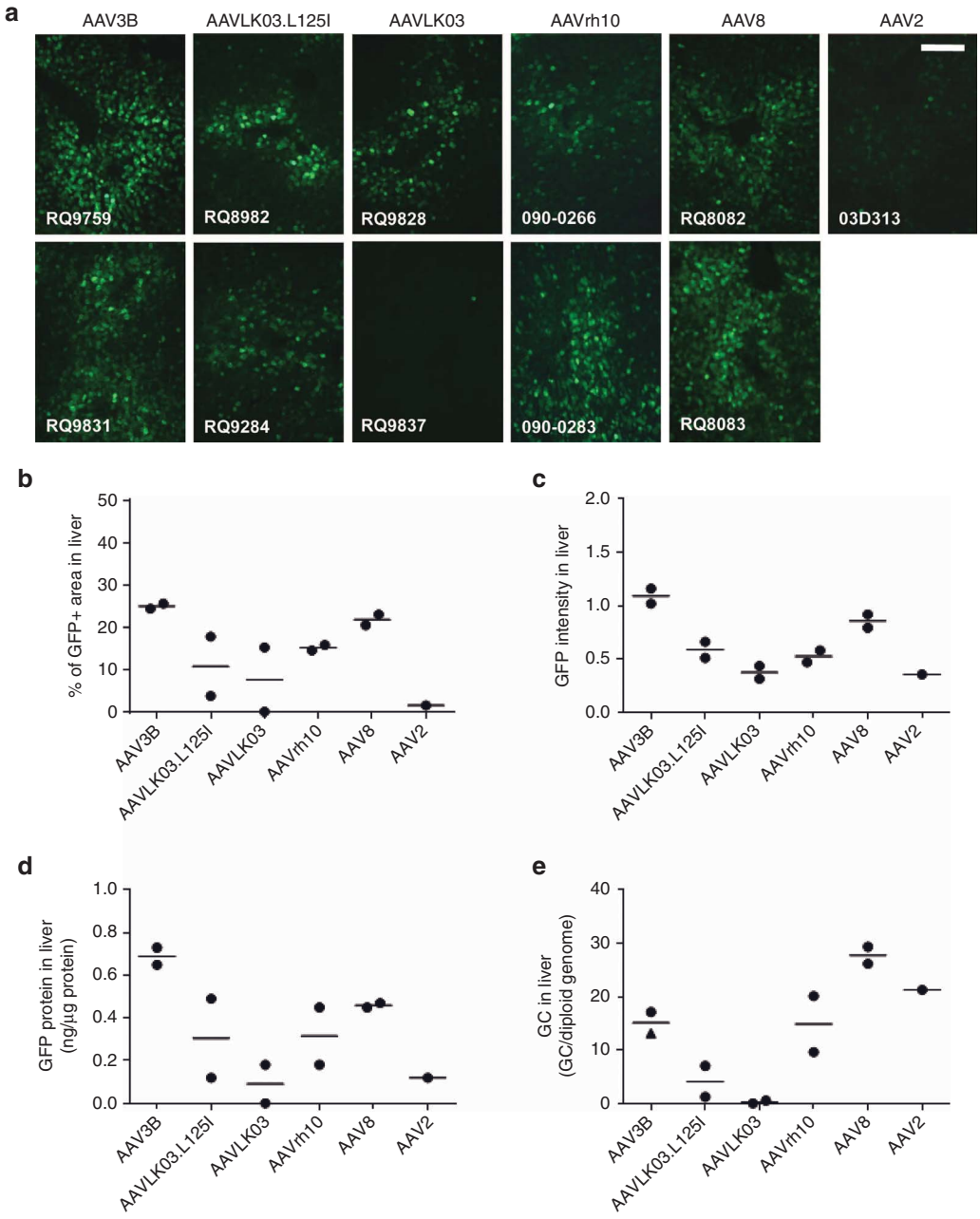

Figure 3 Transduction efficiency (green fluorescent protein (GFP)) in NHP liver. Male rhesus macaques received 3×10^{12} GC/kg of adeno-associated virus (AAV)3B, LK03.L125I, LK03, rh10, AAV8 or AAV2.TBG.GFP vector. Liver was harvested 10 (AAV3B, LK03.L125I, LK03, and AAV2) or 7 days (AAVrh10 and AAV8) postvector administration for GFP expression analysis (**a**). Scale bar: 200 µm. Transduction efficiency in NHP liver was evaluated by (**b**) morphometric analysis of the transduction efficiency based on percent transduction of hepatocytes, (**c**) morphometric analysis of the transduction efficiency based on relative GFP intensity, (**d**) quantification of GFP protein concentration in liver lysate by enzyme-linked immunosorbent assay, and (**e**) vector genome copies in liver. *Note: data on AAV8 (previously published) are included for comparison purpose.[35]

There was excellent correlation of human hepatocyte transduction with all vectors when comparing measures of transduction efficiency using the two different analytical methods. The average transduction efficiencies of human hepatocytes were as follows (% transduction by flow/% transduction by histology): AAV3B – 23/23; AAVLK03 and AAVLK03.L125I – 30/31; AAV8 – 47/27; and AAVrh10 – 41/29. High correlation between the two methods of quantitation was noted with mouse hepatocytes with the exception of some animals receiving clade E vectors where histological analyses yielded higher estimates of transduction for reasons that are unclear but could relate to gating parameters. The relatively high level of transduction of human hepatocytes that was achieved with AAV8 is not consistent with the findings of Lisowski *et al.*[26], who claimed that transduction of human hepatocytes with AAV8 was reduced 20-fold relative to AAVLK03 using the same human liver xenograft model and a similar method of histochemical quantitation of GFP. Specifically, transduction of human hepatocytes in the xenograft model in Lisowski *et al.* was

Sarepta Exhibit 1071, page 4

© The American Society of Gene & Cell Therapy

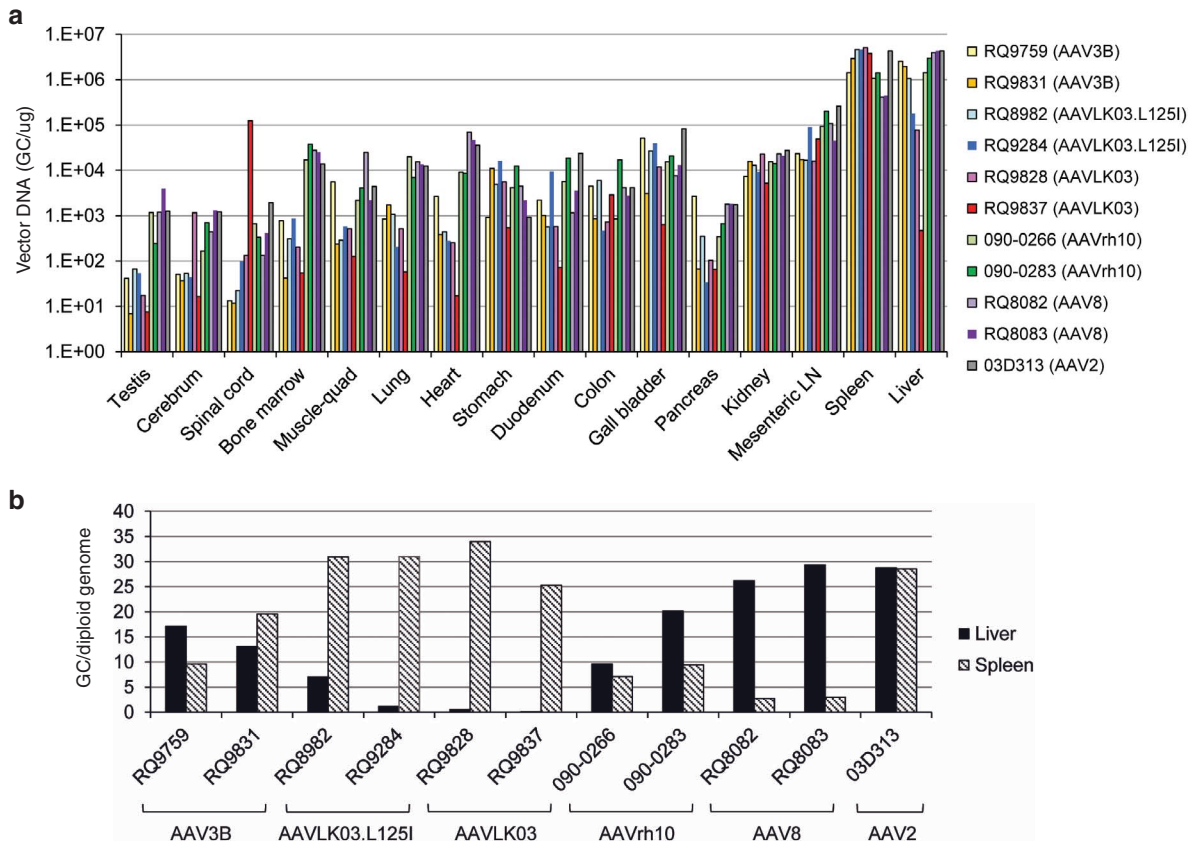

Figure 4 Biodistribution of adeno-associated virus (AAV) vector DNA in tissues of rhesus macaques following intravenous infusion of AAV3B, LK03.L125I, LK03, rh10, AAV8, and AAV2. Tissues were harvested 10 (AAV3B, LK03.L125I, LK03, and AAV2) or 7 days (AAVrh10 and AAV8) post vector administration, total DNA prepared, and AAV DNA quantified by Taqman polymerase chain reaction. (**a**) The data are presented as vector DNA copies per microgram of total DNA. (**b**) Vector genome copies in liver and spleen are also presented as vector DNA copies per diploid genome.

43.3 and 3.6% with AAVLK03 and AAV8, respectively, while in our analyses it was 24 and 27% based on histological analysis and 31 and 46% based on flow cytometry. Lisowski *et al.*[26] also claimed that AAVLK03 is more efficient than AAV3B in the human liver xenograft model based on luciferase imaging, although their data were based on three animals (one for AAV3B and two for AAVLK03) showing only a 2.3-fold difference. Our studies indicate no significant difference between the AAVLK03 (24%), AAVLK03.L125I (37%), and AAV3B (23%) based on histological analysis with similar results using flow cytometry to quantify transduction.

Male rhesus macaques were injected IV with the AAVrh10, AAV3B, AAVLK03, and AAVLK03.L125I vectors expressing GFP (N = 2/vector) and 7–10 days later were necropsied and tissues were evaluated for expression and distribution of vector. These time points were selected to assure peak expression of the transgene before confounding cellular immune responses were activated. One animal was infused with an AAV2-based vector to provide context for earlier preclinical and clinical studies when this capsid was the only one available for *in vivo* studies. Animals were prescreened to assure they did not have pre-existing neutralizing antibodies (NAb) to the capsid of the vector that they received. Previously published data from AAV8.TBG.GFP injected animals (N = 2, RQ8082 and RQ8083) are included for comparison.[35] All animals tolerated vector infusion without any clinical sequelae or abnormalities in blood hematology or chemistry (data not shown). A summary of the macaque studies is provided in **Table 2**.

Liver tissue sections were visualized for transduction by fluorescence microscopy (**Figure 3a**) and quantified for transgene expression by measuring % transduction (surface area of GFP fluorescence within the section, **Figure 3b**) and GFP intensity (**Figure 3c**). Liver homogenates were also analyzed by ELISA for GFP protein (**Figure 3d**). Total vector genomes were measured by qPCR (**Figure 3e**). The relative efficacy of transduction and gene transfer varied between capsids, but in most cases was consistent between the two animals within a group. The hierarchy of performance was the same independent of how it was measured: AAV3B>AAV8>AAVrh10>AAVLK03=AAVLK03.L125I>AAV2. The efficiency of transduction was in excess of 20% of hepatocytes for both AAV3B and AAV8 with vector genomes in excess of 10 copies/diploid genomes for AAVrh10, AAV8, and AAV3B. One animal within the AAVLK03 group had virtually no detectable transduction or gene transfer. It was subsequently learned that this macaque seroconverted to AAVLK03 between the time of screening and dosing (*i.e.*, NAb <1:5 6 weeks prior and 1:20 at time of dosing). Eliminating this animal from the analyses does not change the conclusions. This finding does reinforce the impact that pre-existing immunity can have on the efficacy of liver gene therapy; previous studies with AAV8 in macaques demonstrated a substantial reduction in transduction at

Sarepta Exhibit 1071, page 5

© The American Society of Gene & Cell Therapy

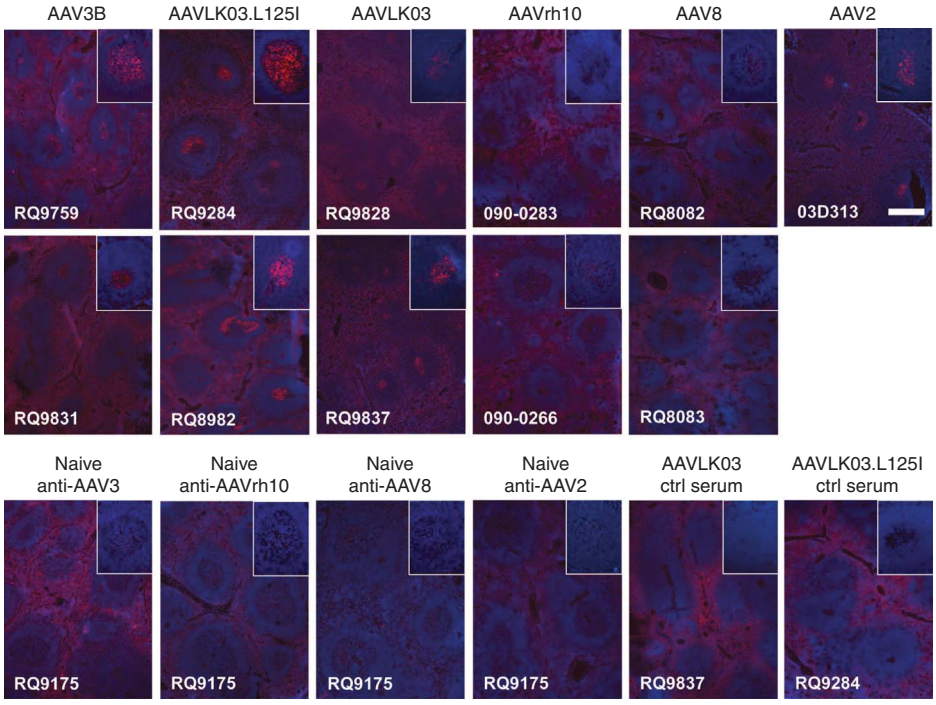

Figure 5 Detection of adeno-associated virus (AAV) capsid within germinal centers of spleen by immunofluorescence (red) following systemic administration of AAV. Sections were counterstained with DAPI (4′,6-diamidino-2-phenylindole, blue) to outline splenic structure. Inset shows germinal center at higher magnification. Serotype-specific antisera were also used to stain spleen from a naïve animal or were omitted as control (RQ9175, lower panel). Scale bar: 400 µm.

titers of NAb in excess of 1:10, which appears to be relevant to vectors of the AAV3-related family.[35]

A number of other studies have attempted to measure transduction efficiency in nonhuman primate liver following IV administration of AAV8 vectors using factor IX as a transgene.[36,37] While it is difficult to compare transduction efficiencies between studies due to a large number of variables such as promoter, method of production, pre-existing immunity, etc., it is interesting to note that the level of human factor IX described in Nathwani *et al.* of 26% of normal was similar to the 20% transduction efficiency we measured with GFP in nonhuman primates, but higher than the levels of human factor IX measured by Mingozzi *et al.* in AAV8-treated nonhuman primates, which had low-titer NAbs.

A more extensive analysis of tissues for biodistribution of vector genomes was conducted (**Figure 4a**). The data were virtually indistinguishable between the two clade E based vectors—AAV8 and AAVrh10—as well as the one animal who received an AAV2 vector. The profiles of vector distribution were also indistinguishable between the AAV3-related vectors (*i.e.*, AAV3B, AAVLK03, and AAVLK03.L125I), although there were substantial differences between clade E/AAV2 vectors and AAV3-related vectors. With all vectors, liver and spleen harbored the highest level of vector, although substantially more vector was directed to spleen from the AAV3-related vectors. Furthermore, most other tissues contained higher levels of clade E vectors than the AAV3-related vectors. These clade-specific differences in liver and spleen vector distribution is highlighted in **Figure 4b**; the ratio of liver to spleen vector genomes was 5.7 for clade E vectors (range 1.3–9.8) and 0.5 for AAV3-related vectors (range 0.02–1.8, excluding RQ9837). It is interesting that the ratio of GFP expression over vector genomes in liver was higher with AAV3-related vectors as compared with clade E vectors. In virtually all AAV liver gene therapy studies, the level of resident genomes is higher than what is predicted by transduction efficiency as measured by histological detection.[13,35,36] We believe this is due primarily to limited sensitivity of most cell-based transgene product assays that underestimate transduction efficiency, although the presence of genomes in liver that are not active is entirely possible.[38] Capsid could play a role in the proportion of inactive genomes by directing them to nonparenchymal liver cells or to portions of the cell not capable of transcription such as in the cytoplasm.

Spleen tissue was further analyzed for presence of capsid protein by immunofluorescence with capsid-specific antibodies (**Figure 5**). Substantial quantities of capsid localized to splenic germinal centers following injection of the AAV3-related vectors. Interestingly, this was not observed in spleen tissue from animals injected with clade E vectors. Within the AAV3 family, vector genomes and germinal center capsid protein was slightly higher with AAVLK03 and AAVLK03.L125I as compared with AAV3B. There was no detectable GFP protein in spleen, presumably due to the fact that its expression was driven by a liver-specific promoter.

A potential impediment to successful liver gene therapy is antibody-mediated inhibition of *in vivo* transduction. NAbs can form from natural AAV infections or from a previous AAV treatment. We surveyed serum from 28 healthy subjects from North America for NAbs to the clade E and AAV3-related vectors evaluated in this study (**Figure 6a**). In this cohort, there was essentially no difference in the prevalence of NAb titers greater than 1:10, which is the threshold we previously showed for AAV8 that was associated with substantial reductions in gene transfer in macaques.[35]

Sarepta Exhibit 1071, page 6

© The American Society of Gene & Cell Therapy

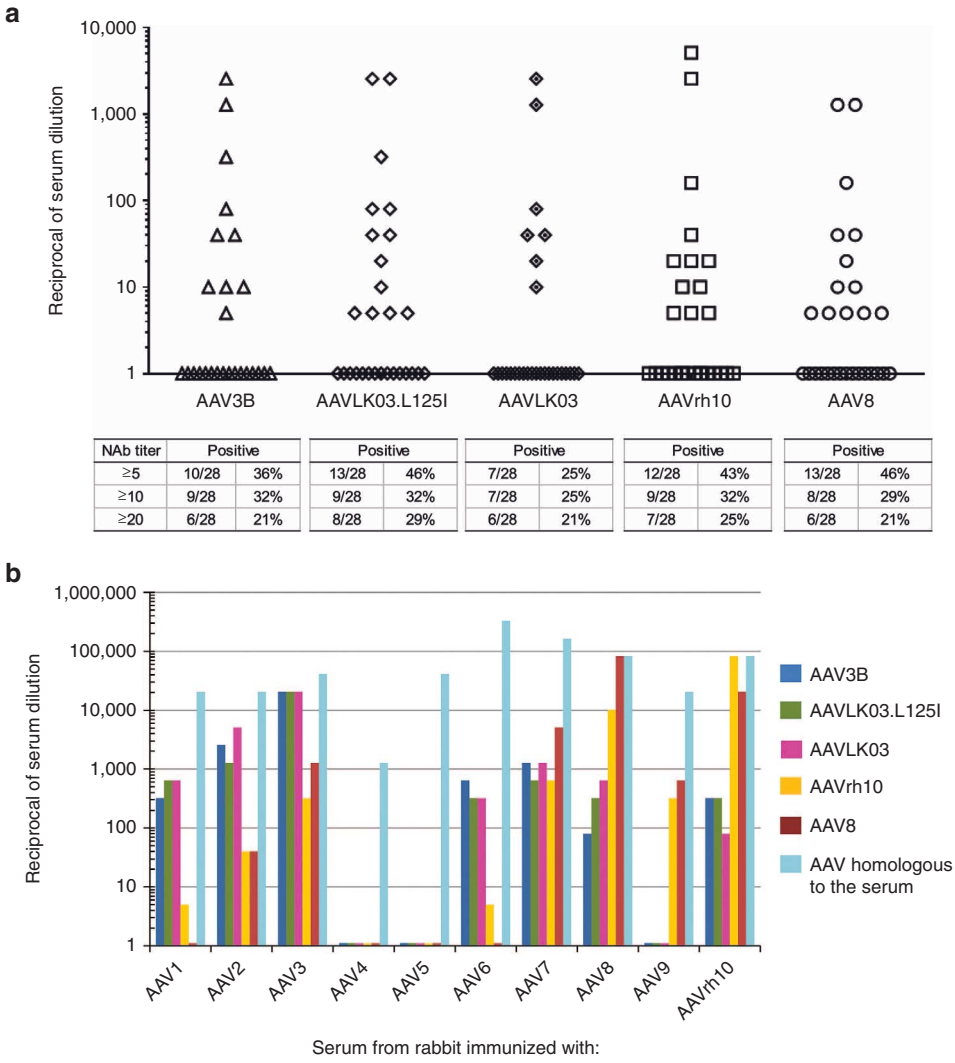

NAb titer	Positive		Positive		Positive		Positive		Positive	
≥5	10/28	36%	13/28	46%	7/28	25%	12/28	43%	13/28	46%
≥10	9/28	32%	9/28	32%	7/28	25%	9/28	32%	8/28	29%
≥20	6/28	21%	8/28	29%	6/28	21%	7/28	25%	6/28	21%

Figure 6 Profiles of neutralizing antibodies. (**a**) Prevalence of neutralizing antibodies against AAV3B, LK03.L125I, LK03, AAVrh10, and AAV8 viruses was determined by an *in vitro* neutralization assay using AAV3B, AAVLK03.L125I, AAVLK03, AAVrh10, and AAV8.CMV.LacZ vectors. Sera from 28 normal human subjects from the United States were tested for their ability to neutralize the transduction of each of the AAV viruses as described in Materials and Methods. (**b**) Cross reactivity of neutralizing antibodies of known AAVs (AAV1-9 and AAVrh10) to AAV3B, LK03.L125I, LK03, rh10, and AAV8. Rabbits were immunized with intramuscular injections of 1×10^{13} GC of each of the AAV serotypes and boosted 34 days later with the same dose. Sera were analyzed for the presence of neutralizing antibodies by incubating serial twofold dilutions with 1×10^{9} GC of each appropriate AAV vector expressing LacZ. The serum dilution that produced a 50% reduction of LacZ expression was scored as the neutralizing antibody titer against that particular virus.

These vectors were also evaluated for cross neutralization with sera generated in rabbits to the individual capsids. **Figure 6b** presents the ability of sera generated to AAV1 – AAV9 and AAVrh10 to neutralize the clade E and AAV3-related vectors that are the subject of this study. As expected, there was a high degree of cross neutralization within the clade E vectors as well as within the AAV3-related vectors, although neutralization was substantially diminished when evaluated across clades/families. For example, sera generated to AAV8 neutralized the AAV3-related vectors at titers that were reduced three logs compared with titer achieved against itself. A similar reduction in neutralizing titers to AAV3-related vectors was observed with sera generated to the other AAVs currently used in clinical trials (AAV9 and AAVrh10) as compared with the effectiveness of the sera to neutralize the capsid to which the sera were generated.

DISCUSSION

Liver-directed gene therapy has advanced into the clinic on multiple fronts for hemophilia B.[6,15,16] The first clinical trial used AAV2, which did not progress beyond phase 1 due to low level and transient expression of factor IX concurrent with liver toxicity.[6] Based on promising preclinical studies in mice and monkeys, several groups conducted clinical trials with AAV8-based vectors in patients with hemophilia B. The St. Jude's/UCL trial achieved low level but stable expression of factor IX without dose limiting toxicities that has substantially reduced or eliminated the need for traditional protein replacement treatments.[15,16] These seminal

© The American Society of Gene & Cell Therapy

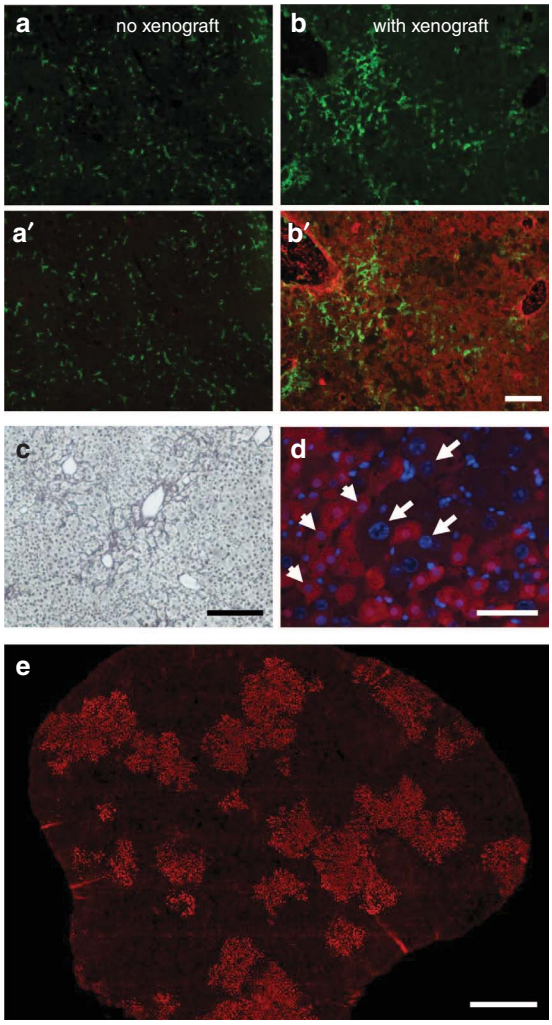

Figure 7 Histopathology of livers from FRG mice engrafted with human hepatocytes. Staining of Kupffer cells with F4/80 antibody on liver sections from FRG mice without (**a**) and with (**b**) human xenograft. Corresponding images (**a′**, **b′**) showing Kupffer cell staining (green) together with staining for human albumin (red) as a marker for human hepatocytes. In the liver engrafted with human hepatocytes, Kupffer cells tend to be focally concentrated. Scale bar: 300 µm. (**c**) Reticulin stain plus hematoxylin stain for nuclei of a liver section from an FRG mouse engrafted with human hepatocytes showing abnormal liver architecture. Note different sizes of hepatocytes. Scale bar: 200 µm. (**d**) DAPI staining together with immunostaining for human fumarylacetoacetase (hFAH) of an engrafted liver of an FRG mouse demonstrating the larger size of murine hepatocytes (arrows) compared with human hepatocytes (arrowheads). Scale bar: 100 µm. (**e**) FRG mouse liver section stained for hFAH demonstrating the nodular growth pattern of human hepatocytes. Scale bar: 3 mm.

human proof-of-concept studies bode well for the use of AAV8 vectors in other liver-based diseases.

We are interested in developing next-generation AAV vectors for liver gene therapy for several reasons. Further improvements in transduction efficiency would expand the scope of candidate diseases and may achieve enhanced clinical efficacy in the more challenging disease targets. Strategies for assuring a second administration of an AAV vector could be achieved with a liver-tropic vector that is serologically distinct from AAV8.

Our initial focus in this study was to evaluate vectors based on capsids isolated from natural sources (AAVrh10 and AAV3B). To do so, we deployed the full spectrum of *in vitro* and *in vivo* models including standard mouse strains, immune-deficient mice with livers partially repopulated with human hepatocytes, and nonhuman primates.

Studies with vectors based on the clade E capsid, AAVrh10, indicated high liver tropism without substantive toxicity in all *in vivo* models studied that was indistinguishable from the data generated with AAV8. We conclude that AAVrh10 is an adequate substitute for AAV8 in first-line liver-directed gene therapy trials. AAVrh10 would not be a useful vector for readministration following an AAV8 treatment due to high sequence similarity with AAV8 and the corresponding serologic cross reactivity.

Vectors based on AAV3B yielded very interesting profiles of activities. The extremely low transduction achieved in mice *in vivo* with AAV3B vectors complicated their experimental development since most of the disease models are in mice. The work of Srivastava and colleagues demonstrated high transduction of human hepatoma cell lines with AAV3 vectors, which compelled us to further pursue this capsid for human liver gene therapy with some reservation since *in vitro* transduction generally does not predict *in vivo* transduction.[28] Our studies indicated that AAV3B vectors are capable of very high *in vivo* transduction of human hepatocytes in the human liver xenograft model and in monkey hepatocytes in the macaque liver. An important difference between AAV3B and the clade E vectors was in their biodistribution in nonhuman primates. Both vectors efficiently transduce liver, although substantially higher quantities of AAV3B vector were trafficked to spleen as compared with AAV8 and AAVrh10, and lower quantities of AAV3B vector were directed to tissues outside of liver and spleen versus what was observed with AAV8 and AAVrh10. This enhanced trafficking of AAV3B to spleen did not appear to increase toxicity. AAV3B vectors could be considered as alternative options to clade E vectors in first-line applications, although their most significant value may be in readministration following an initial treatment with a clade E vector.

The engineered capsid AAVLK03 was isolated by Lisowski *et al.*[26] following DNA shuffling and selection in the human liver xenograft model. They assert that AAVLK03 vectors are substantially more efficient than AAV8 and AAV3B vectors for human liver gene therapy based on the studies in the human liver xenograft model. Our studies indicate that vectors based on AAVLK03 and AAVLK03.L125I are indistinguishable from AAV3B in all model systems, including nonhuman primates, which is not surprising considering the high degree of homology between these capsids and, as shown by Lisowski *et al.*,[26] that AAVLK03 and AAV3B are internalized by the same coreceptor. Furthermore, our studies in the human liver xenograft model showed equally high levels of transduction with AAVLK03 and AAV8; findings which were confirmed in nonhuman primates and extended to include biodistribution.

In an attempt to understand the basis for such divergent conclusions regarding the potential of AAV for human liver gene therapy, we evaluated the strengths and limitations of the human liver xenograft model which Lisowski *et al.* relied on. Our experience with human liver xenograft mice from multiple academic

Sarepta Exhibit 1071, page 8

© The American Society of Gene & Cell Therapy

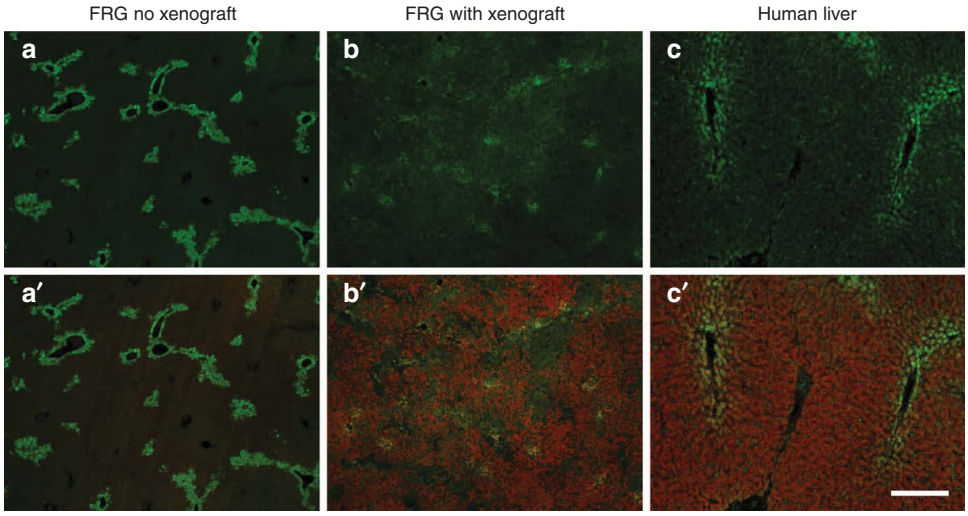

Figure 8 Staining of liver sections with antibodies against glutamine synthetase (GS), a marker for pericentral hepatocytes. Shown are the liver from an FRG mouse without xenograft (**a**), a liver from an FRG mouse repopulated with human hepatocytes (**b**), and a human liver (**c**). Panels **a′**–**c′** show corresponding images with double staining for GS (green) and human fumarylacetoacetase as a marker for human cells (red). Pericentral hepatocytes are no longer clearly detectable in the xenograft liver, indicating disruption of pericentral organization. Scale bar: 400 µm.

laboratories and one commercial source is consistent with the literature in that "repopulation" of the mouse liver is incomplete and occurs in what appears to be nodular outgrowths of human cells (**Figure 7e**).[32] These nodules perturb the normal architecture of the liver, as demonstrated by histological inspection of reticulin-stained paraffin sections (**Figure 7c**), as well as the distribution and structure of key vascular structures such as central veins visualized by staining for glutamine synthetase (**Figure 8**). Also, the density and localization of nonparenchymal cells such as Kupffer cells are frequently abnormal (**Figure 7a**,**b**). Finally, the human hepatocytes are much smaller than adjacent mouse hepatocytes (**Figure 7d**). These differences and pathologies, which vary from animal to animal in proportion to the extent of nodularity, could impact on transduction profiles by perturbing the dynamics of micro and macro vascular perfusion and modifying the function of repopulated hepatocytes. The variable presence of mouse hepatocytes could confound the study of human hepatocyte transduction by competing for uptake if the vectors being compared differ with respect to mouse hepatocyte transduction, as is the case for clade E versus AAV3-related vectors. One aspect of the model which likely impacts on repopulation and transduction efficiency is the source of donor hepatocytes. Lisowski *et al.*[26] used the same source for the selection experiments, although multiple sources were used to generate the human liver xenograft mice used to study the performance of different vectors. A single source of hepatocytes was used to create the 12 human liver xenograft mice in our study. In order to realize the full potential of the human liver xenograft model, it will be important to better understand the impact of donor cells on the biology of AAV transduction and/or identify a universal source of donor cells.

Despite the challenges of the human liver xenograft models noted above, this model could be useful in progressing human gene therapy research. We recently created a mouse model of familial hypercholesterolemia by repopulating the liver of an FRG mouse with hepatocytes derived from a familial hypercholesterolemia patient.[39] The utility of this approach in developing models of human liver diseases would be markedly expanded if human-derived iPS cells would repopulate the FRG mouse liver. Until we better understand factors that contribute to animal-to-animal variation in human hepatocyte repopulation in the FRG mouse, one should be careful in interpreting comparative studies of vector biology across different animals. We do see a role, however, in using the human liver xenograft model to evaluate relative performance of, and possible selection for, populations of vectors within individual mice such as in the identification of antibody escape mutants in animals passively transferred with human serum.

A key question that remains is what is the best preclinical model for predicting successful AAV gene therapy in the clinic? Establishing function of the gene therapy product in terms of ameliorating pathology requires animals that mimic the phenotype of the disease, which is usually a mouse model–although, in selected cases, larger animal models are available such as in dogs and cats. The human liver xenograft has the potential to evaluate tropism of the capsid for human hepatocytes, however, the efficacy and safety of *in vivo* transduction is impacted by factors other than the interaction of the vector with the target cell. Confounding factors include competitive uptake by extrahepatic organs such as spleen, interaction with plasma proteins, and innate and adaptive immune responses, many of which can be studied in nonhuman primates.

MATERIALS AND METHODS

Vectors. AAV vectors AAV3B, AAVLK03, AAVLK03.L125I, and AAVrh10 carrying the TBG.GFP.bGH or CMV.LacZ.bGH cassettes were produced by the Vector Core at the University of Pennsylvania as previously described in which vector is recovered from the supernatant and purified on an iodixanol gradient.[40] AAV2 was recovered from total cell lysate and purified by two rounds of CsCl gradient. Vectors for macaque studies were subjected to extensive quality control tests including three repeated vector genome titrations based on qPCR, sodium dodecyl sulfate–polyacrylamide gel electrophoresis (SDS–PAGE) analysis for vector purity, Limulus amebocyte lysate for endotoxin detection (Cambrex Bio Science, East

© The American Society of Gene & Cell Therapy

Rutherford, NJ), and transgene expression analysis in mice. All vectors used in the nonhuman primate studies were isolated with high yield and were free of endotoxin with greater than 94% purity based on SDS-PAGE.

Murine experiments. All mice were housed in an AAALAC (Association for Assessment and Accreditation of Laboratory Animal Care)-accredited and Public Health Service-assured facility at the University of Pennsylvania, and all animal procedures were performed in accordance with protocols approved by the Institute of Animal Care and Use Committees (IACUC) at the University of Pennsylvania. C57BL/6 male mice (6–8 weeks old) were purchased from Jackson Laboratories (Bar Harbor, ME) and received a single tail vein injection of 1×10^{11} or 3×10^{11} genome copies of vector. GFP expressions were evaluated 2 weeks postvector injection. Male FRG mice on a C57BL/6N background and repopulated with 40–70% human hepatocytes, were purchased from Taconic-Yecuris (Tualatin, OR). All 12 mice were repopulated with hepatocytes derived from the same donor which was a 17 YO Caucasian female. Mice were provided ad libitum access to irradiated Purina Lab Diet 5LJ5 (Ralston Purina, St. Louis, MO). According to the vendor's recommendations, all animals were initially maintained on a sterile solution of Nitisinone (NTBC, 8 mg/l, Yecuris, Tualatin, OR) and supplemented with Sulfamethoxazole (SMX, 640 mg/l; Yecuris) plus Trimethoprin (TMP, 128 mg/l, Yecuris) in 3% dextrose drinking water. Two weeks before vector administration, NTBC was withdrawn and animals were maintained on 3% dextrose drinking water supplemented with SMX/TMP. AAV.TBG.GFP vector (3×10^{11} GC) was intravenously administered and animals were put back on NTBC 1 week later. During NTBC withdrawal, mice that became dehydrated and/or lost ≥10% of their preshipment body weight were treated with fluid intervention and high-calorific diet (STAT, PRN Pharmacal, Pensacola, FL). Livers and hepatocytes were isolated 3 weeks post vector infusion.

Macaque experiments. Juvenile rhesus macaques (male Chinese origin and captive bred) were treated and cared for at an AAALAC-accredited and Public Health Service-assured facility at the University of Pennsylvania (Philadelphia, PA) during the study. The study was performed according to a protocol approved by the Environmental Health and Radiation Safety Office, the Institutional Biosafety Committee, and the IACUC of the University of Pennsylvania. Vectors (3×10^{12} GC/kg) were administered to the study animals via the saphenous vein in a total volume of 10 ml infused at 1 ml per minute using a Harvard infusion pump. Blood samples were taken prestudy and at the time of necropsy via venipuncture of the femoral vein. At the time of necropsy, the target organ liver and 15 distant tissues (cerebrum, spinal cord, heart, lung, gallbladder, pancreas, spleen, kidney, testicles, stomach, duodenum, colon, mesenteric lymph nodes, bone marrow, and skeletal muscle-quadriceps femoris) were collected for vector biodistribution analysis.

Histology. To visualize GFP fluorescence, liver tissues were fixed overnight in formalin, washed in phosphate-buffered saline, and frozen in optimum cutting temperature (OCT) compound (Sakura Finetek, Torrance, CA) to produce cryosections (8 µm). GFP-positive liver area was quantified on representative images of cryosections from each animal (10× objective; 10 images for each nonhuman primate (NHP) and a minimum of 3 images for each group of mice) using ImageJ software (W. Rasband, National Institutes of Health, Bethesda, MD; http://rsb.info.nih.gov/ij). Images were set to a threshold to select GFP-positive hepatocytes and the percentage of GFP-positive liver area was then determined and averaged for each NHP or group of mice.

Liver sections from NHPs were further analyzed by measuring the fluorescence intensity of GFP. GFP intensity was measured as the total intensity of every image (*i.e.*, the sum of all pixel values per image) determined with ImageJ software. The resulting intensity values were then calculated as a fraction of a fluorescence standard,[41] *i.e.*, a 10% (w/v) solution of sodium fluorescein (Sigma-Aldrich, St. Louis, MO) in 0.1 M $NaHCO_3$. Images were taken from the reference solution spread on a slide and the original GFP intensity values were then divided by the reference values to obtain the final GFP intensity value. For each liver, 10 images were analyzed and mean values are presented.

Immunostaining on spleen sections was performed as described using rabbit sera made in our laboratory against the described serotypes.[35] AAVLK03 and LK03.L125I were detected using a rabbit serum raised against AAV3B.

Immunostaining on livers of xenograft mice was performed on formalin-fixed paraffin-embedded liver tissues. Paraffin sections were dewaxed and antigen retrieval was performed in citrate buffer pH6.0. Incubation with primary antibodies was performed after blocking with 1% donkey serum + 0.2% Triton using chicken antibodies against GFP (Abcam, Cambridge, MA) and goat antibodies against FAH (Santa Cruz, Dallas, TX). After washing in phosphate-buffered saline, the sections were stained with fluorescent-labeled secondary antibodies (Jackson Immunoresearch Laboratories, West Grove, PA) in 1% donkey serum for 30 minutes, washed again, and mounted with Vectashield plus DAPI (Vector Labs, Burlingame, CA).

To quantify percentages of transduced human and mouse hepatocytes, 10 images (10× objective) from each xenograft liver were taken for each channel (GFP and FAH stain). The percentage of image area positive for each protein was determined by thresholding with ImageJ software. Next, the thresholded images showing GFP expression were combined with the corresponding thresholded images showing human hepatocytes (*i.e.*, FAH-positive area) or mouse hepatocytes (*i.e.*, FAH-negative area not including cell-free areas such as veins). This was achieved with ImageJ's "Image Calculator" tool by image addition of tresholded images where the thresholded pixels equal 0 and the nonthresholded pixels equal 255 (so that 0 + 0 = 0, *i.e.*, only the overlap area between two images remains the value 0 in the resulting image). The overlap area (*i.e.*, pixels with value 0 showing GFP-positive human or mouse cells) was then quantified and the percentage of GFP-positive human and mouse cells determined.

Further analyses of livers for histopathology was performed by immunostaining as described above using antibodies against glutamin synthetase (rabbit antibody, 1:100, Abcam, Cambridge, MA), Kupffer cells (F4/80, 1:200, Serotec/Bio-Rad, Hercules, CA), and human albumin (goat antibodies, 1:200, Bethyl, Laboratories, Montgomery, TX). Reticulin staining was performed with a kit from Sigma. DAPI staining was obtained by using Vectashield with DAPI as mounting medium.

Hepatocyte isolation and flow cytometry. Mouse hepatocytes were isolated in a BSL-2 hood based on the *in situ* two-step collagenase perfusion technique.[41,42] Briefly, the animal was anesthetized and opened up to expose the lower abdomen. The inferior vena cava was perfused for 5 minutes (retrograde perfusion) with Liver perfusion medium (Thermo Fisher Scientific, Waltham, MA). Once the perfusion was started the portal vein was cut to allow outflow of the perfusion. After 5 minutes, the buffer was changed to collagenase medium containing 0.8 mg/ml Collagenase Type I (Worthington, Biochemical, Lakewood, NJ) in Hanks balanced salt solution and perfused for an additional 12 minutes. The collagenase and perfusion buffers were maintained in a water bath set at 39 °C. At the end of the perfusion, the liver was excised and placed in Hepatocyte wash medium (Thermo Fisher Scientific) and the hepatocytes gently dispersed by teasing the tissue. The hepatocyte preparation was filtered through a 100 micron filter and washed three times and resuspended in hepatocyte wash medium.

For flow cytometry analysis, 1 million hepatocytes were stained with PE-Cy7 conjugated anti-human HLA-A,B,C (BD Biosciences, San Jose, CA) and Alexa 647 conjugated anti-mouse H2-k^b (BD biosciences). Stained cells were washed and evaluated for percent transduced human or mouse hepatocytes by gating on the GFP^+ HLA^+ or GFP^+ H2-K^{b+} cells, respectively. Samples were run on a Beckman Coulter flow cytometer (FC500) and the data analyzed using FlowJo (Tree Star, Ashland, OR).

Quantification of GFP protein in liver lysate. GFP protein concentration in macaque liver lysate was measured by ELISA as previously described.[35]

© The American Society of Gene & Cell Therapy

Vector biodistribution analysis. Tissue DNAs were extracted using QIAamp DNA Mini Kit (Qiagen, Valencia, CA). Detection and quantification of vector genomes in extracted DNA were performed by real-time PCR as described previously.

AAV-neutralizing antibody assay. Serum samples were collected and AAV NAb assays were performed on Huh7 cells as previously described.[43] The limit of detection for the assay is 1:5 serum dilution.

SUPPLEMENTARY MATERIAL

Figure S1. *In vitro* transduction efficiency on Huh7 cells. Huh7 cells were co-infected with wild type adenovirus (MOI=45) and AAV3B, LK03.L125I, LK03, rh10 or AAV8.CMV.LacZ vectors at the MOI of 1,000 (solid bar) and 10,000 (hatched bar).

ACKNOWLEDGMENTS

The authors thank Penn Vector Core, University of Pennsylvania Perelman School of Medicine, Gene Therapy Program for supplying vectors; Rebecca Grant and Erin Bote, University of Pennsylvania Perelman School of Medicine, Gene Therapy Program for invaluable assistance with macaque studies; Christine Draper, Qiuyue Qin, Surina Boyd, Mark Schneider, University of Pennsylvania Perelman School of Medicine Gene Therapy Program, for technical assistance. This work was supported by NIH grants: NICHD P01-HD057247 (J.M.W.), NHLBI P01-HL059407 (J.M.W.), and NIDDK P30-DK047757 (J.M.W.). J.M.W. is an advisor to REGENXBIO, Dimension Therapeutics, Solid Gene Therapy, and Alexion, and is a founder of, holds equity in, and has a sponsored research agreement with REGENXBIO and Dimension Therapeutics; in addition, he is a consultant to several biopharmaceutical companies and is an inventor on patents licensed to various biopharmaceutical companies.

REFERENCES

1. Hastie, E and Samulski, RJ (2015). Adeno-associated virus at 50: a golden anniversary of discovery, research, and gene therapy success–a personal perspective. *Hum Gene Ther* **26**: 257–265.
2. Snyder, RO, Miao, CH, Patijn, GA, Spratt, SK, Danos, O, Nagy, D *et al.* (1997). Persistent and therapeutic concentrations of human factor IX in mice after hepatic gene transfer of recombinant AAV vectors. *Nat Genet* **16**: 270–276.
3. Wang, L, Takabe, K, Bidlingmaier, SM, Ill, CR and Verma, IM (1999). Sustained correction of bleeding disorder in hemophilia B mice by gene therapy. *Proc Natl Acad Sci USA* **96**: 3906–3910.
4. Nathwani, AC, Davidoff, AM, Hanawa, H, Hu, Y, Hoffer, FA, Nikanorov, A *et al.* (2002). Sustained high-level expression of human factor IX (hFIX) after liver-targeted delivery of recombinant adeno-associated virus encoding the hFIX gene in rhesus macaques. *Blood* **100**: 1662–1669.
5. Mount, JD, Herzog, RW, Tillson, DM, Goodman, SA, Robinson, N, McCleland, ML *et al.* (2002). Sustained phenotypic correction of hemophilia B dogs with a factor IX null mutation by liver-directed gene therapy. *Blood* **99**: 2670–2676.
6. Manno, CS, Pierce, GF, Arruda, VR, Glader, B, Ragni, M, Rasko, JJ *et al.* (2006). Successful transduction of liver in hemophilia by AAV-Factor IX and limitations imposed by the host immune response. *Nat Med* **12**: 342–347.
7. Mingozzi, F, Schüttrumpf, J, Arruda, VR, Liu, Y, Liu, YL, High, KA *et al.* (2002). Improved hepatic gene transfer by using an adeno-associated virus serotype 5 vector. *J Virol* **76**: 10497–10502.
8. Grimm, D, Zhou, S, Nakai, H, Thomas, CE, Storm, TA, Fuess, S *et al.* (2003). Preclinical *in vivo* evaluation of pseudotyped adeno-associated virus vectors for liver gene therapy. *Blood* **102**: 2412–2419.
9. Xiao, W, Chirmule, N, Berta, SC, McCullough, B, Gao, G and Wilson, JM (1999). Gene therapy vectors based on adeno-associated virus type 1. *J Virol* **73**: 3994–4003.
10. Ylä-Herttuala, S (2012). Endgame: glybera finally recommended for approval as the first gene therapy drug in the European union. *Mol Ther* **20**: 1831–1832.
11. Gao, GP, Alvira, MR, Wang, L, Calcedo, R, Johnston, J and Wilson, JM (2002). Novel adeno-associated viruses from rhesus monkeys as vectors for human gene therapy. *Proc Natl Acad Sci USA* **99**: 11854–11859.
12. Wang, L, Wang, H, Bell, P, McCarter, RJ, He, J, Calcedo, R *et al.* (2010). Systematic evaluation of AAV vectors for liver directed gene transfer in murine models. *Mol Ther* **18**: 118–125.
13. Wang, L, Calcedo, R, Wang, H, Bell, P, Grant, R, Vandenberghe, LH *et al.* (2010). The pleiotropic effects of natural AAV infections on liver-directed gene transfer in macaques. *Mol Ther* **18**: 126–134.
14. Nathwani, AC, Gray, JT, Ng, CY, Zhou, J, Spence, Y, Waddington, SN *et al.* (2006). Self-complementary adeno-associated virus vectors containing a novel liver-specific human factor IX expression cassette enable highly efficient transduction of murine and nonhuman primate liver. *Blood* **107**: 2653–2661.
15. Nathwani, AC, Tuddenham, EG, Rangarajan, S, Rosales, C, McIntosh, J, Linch, DC *et al.* (2011). Adenovirus-associated virus vector-mediated gene transfer in hemophilia B. *N Engl J Med* **365**: 2357–2365.
16. Nathwani, AC, Reiss, UM, Tuddenham, EG, Rosales, C, Chowdary, P, McIntosh, J *et al.* (2014). Long-term safety and efficacy of factor IX gene therapy in hemophilia B. *N Engl J Med* **371**: 1994–2004.
17. NCT01161576. Safety study of a gene transfer vector (Rh.10) for children with late infantile neuronal ceroid lipofuscinosis. https://clinicaltrials.gov/.
18. NCT01414985. AAVRh.10 administered to children with late infantile neuronal ceroid lipofuscinosis with uncommon genotypes or moderate/severe impairment. https://clinicaltrials.gov/.
19. NCT02122952. Gene transfer clinical trial for spinal muscular atrophy type 1. https://clinicaltrials.gov/.
20. Maheshri, N, Koerber, JT, Kaspar, BK and Schaffer, DV (2006). Directed evolution of adeno-associated virus yields enhanced gene delivery vectors. *Nat Biotechnol* **24**: 198–204.
21. Perabo, L, Endell, J, King, S, Lux, K, Goldnau, D, Hallek, M *et al.* (2006). Combinatorial engineering of a gene therapy vector: directed evolution of adeno-associated virus. *J Gene Med* **8**: 155–162.
22. Koerber, JT, Maheshri, N, Kaspar, BK and Schaffer, DV (2006). Construction of diverse adeno-associated viral libraries for directed evolution of enhanced gene delivery vehicles. *Nat Protoc* **1**: 701–706.
23. Grimm, D, Lee, JS, Wang, L, Desai, T, Akache, B, Storm, TA *et al.* (2008). *In vitro* and *in vivo* gene therapy vector evolution via multispecies interbreeding and retargeting of adeno-associated viruses. *J Virol* **82**: 5887–5911.
24. Li, W, Asokan, A, Wu, Z, Van Dyke, T, DiPrimio, N, Johnson, JS *et al.* (2008). Engineering and selection of shuffled AAV genomes: a new strategy for producing targeted biological nanoparticles. *Mol Ther* **16**: 1252–1260.
25. Koerber, JT, Jang, JH and Schaffer, DV (2008). DNA shuffling of adeno-associated virus yields functionally diverse viral progeny. *Mol Ther* **16**: 1703–1709.
26. Lisowski, L, Dane, AP, Chu, K, Zhang, Y, Cunningham, SC, Wilson, EM *et al.* (2014). Selection and evaluation of clinically relevant AAV variants in a xenograft liver model. *Nature* **506**: 382–386.
27. Schmidt, M, Govindasamy, L, Afione, S, Kaludov, N, Agbandje-McKenna, M and Chiorini, JA (2008). Molecular characterization of the heparin-dependent transduction domain on the capsid of a novel adeno-associated virus isolate, AAV(VR-942). *J Virol* **82**: 8911–8916.
28. Cheng, B, Ling, C, Dai, Y, Lu, Y, Glushakova, LG, Gee, SW *et al.* (2012). Development of optimized AAV3 serotype vectors: mechanism of high-efficiency transduction of human liver cancer cells. *Gene Ther* **19**: 375–384.
29. Ling, C, Lu, Y, Cheng, B, McGoogan, KE, Gee, SW, Ma, W *et al.* (2011). High-efficiency transduction of liver cancer cells by recombinant adeno-associated virus serotype 3 vectors. *J Vis Exp* **49**:e2538.
30. Ling, C, Wang, Y, Zhang, Y, Ejjigani, A, Yin, Z, Lu, Y *et al.* (2014). Selective *in vivo* targeting of human liver tumors by optimized AAV3 vectors in a murine xenograft model. *Hum Gene Ther* **25**: 1023–1034.
31. Lisowski, L and Kay, MA (2013). US 2013/0059732 A1. United Patent Application Publication.
32. Bissig, KD, Le, TT, Woods, NB and Verma, IM (2007). Repopulation of adult and neonatal mice with human hepatocytes: a chimeric animal model. *Proc Natl Acad Sci USA* **104**: 20507–20511.
33. Azuma, H, Paulk, N, Ranade, A, Dorrell, C, Al-Dhalimy, M, Ellis, E *et al.* (2007). Robust expansion of human hepatocytes in Fah-/-/Rag2-/-/Il2rg-/- mice. *Nat Biotechnol* **25**: 903–910.
34. Bissig, KD, Wieland, SF, Tran, P, Isogawa, M, Le, TT, Chisari, FV *et al.* (2010). Human liver chimeric mice provide a model for hepatitis B and C virus infection and treatment. *J Clin Invest* **120**: 924–930.
35. Wang, L, Calcedo, R, Bell, P, Lin, J, Grant, RL, Siegel, DL *et al.* (2011). Impact of pre-existing immunity on gene transfer to nonhuman primate liver with adeno-associated virus 8 vectors. *Hum Gene Ther* **22**: 1389–1401.
36. Nathwani, AC, Gray, JT, McIntosh, J, Ng, CY, Zhou, J, Spence, Y *et al.* (2007). Safe and efficient transduction of the liver after peripheral vein infusion of self-complementary AAV vector results in stable therapeutic expression of human FIX in nonhuman primates. *Blood* **109**: 1414–1421.
37. Mingozzi, F, Anguela, XM, Pavani, G, Chen, Y, Davidson, RJ, Hui, DJ *et al.* (2013). Overcoming preexisting humoral immunity to AAV using capsid decoys. *Sci Transl Med* **5**: 194ra92.
38. Wang, L, Morizono, H, Lin, J, Bell, P, Jones, D, McMenamin, D *et al.* (2012). Preclinical evaluation of a clinical candidate AAV8 vector for ornithine transcarbamylase (OTC) deficiency reveals functional enzyme from each persisting vector genome. *Mol Genet Metab* **105**: 203–211.
39. Bissig-Choisat, B, Wang, L, Legras, X, Saha, PK, Chen, L, Bell, P *et al.* (2015). Development and rescue of human familial hypercholesterolaemia in a xenograft mouse model. *Nat Commun* **6**: 7339.
40. Lock, M, Alvira, M, Vandenberghe, LH, Samanta, A, Toelen, J, Debyser, Z *et al.* (2010). Rapid, simple, and versatile manufacturing of recombinant adeno-associated viral vectors at scale. *Hum Gene Ther* **21**: 1259–1271.
41. Model, MA and Burkhardt, JK (2001). A standard for calibration and shading correction of a fluorescence microscope. *Cytometry* **44**: 309–316.
42. Li, WC, Ralphs, KL and Tosh, D (2010). Isolation and culture of adult mouse hepatocytes. *Methods Mol Biol* **633**: 185–196.
43. Calcedo, R, Vandenberghe, LH, Gao, G, Lin, J and Wilson, JM (2009). Worldwide epidemiology of neutralizing antibodies to adeno-associated viruses. *J Infect Dis* **199**: 381–390.
44. Nam, HJ, Lane, MD, Padron, E, Gurda, B, McKenna, R, Kohlbrenner, E *et al.* (2007). Structure of adeno-associated virus serotype 8, a gene therapy vector. *J Virol* **81**: 12260–12271.
45. Pettersen, EF, Goddard, TD, Huang, CC, Couch, GS, Greenblatt, DM, Meng, EC *et al.* (2004). UCSF Chimera–a visualization system for exploratory research and analysis. *J Comput Chem* **25**: 1605–1612.
46. Sanner, MF, Olson, AJ and Spehner, JC (1996). Reduced surface: an efficient way to compute molecular surfaces. *Biopolymers* **38**: 305–320.